Journal of Computer Science and Electrical Engineering
Print ISSN: 2663-1938
Online ISSN: 2663-1946
DOI: https://doi.org/10.61784/jcsee3169

INTERSECTION-LOCALIZATION POLYGON SOLVING AND COVERAGE JUDGMENT FOR RADIO INTERFERENCE SOURCES WITH BOUNDED DIRECTION-FINDING ERRORS

HuChen Zhang[1*], PengJie Peng[2], BoWen Wu[3], HaoRan Dai[4], ZiYan Yu[5], XinChen Wang[1]
[1]*School of Big Data and Artificial Intelligence, Anhui Institute of Information Technology, Wuhu 241100, Anhui, China.*
[2]*School of Engineering Science, University of Science and Technology of China, Hefei 230026, Anhui, China.*
[3]*School of Electrical and Electronic Engineering, Anhui Institute of Information Technology, Wuhu 241100, Anhui, China.*
[4]*College of Environmental and Resource Sciences and College of Carbon Neutral Modern Industry, Fujian Normal University, Fuzhou 350117, Fujian, China.*
[5]*School of Computer and Information Engineering, Chuzhou University, Chuzhou 239000, Anhui, China.*
[*]*Corresponding Author: HuChen Zhang*

Abstract: Aiming at the localization problem of radio interference sources under bounded angular errors of direction-finding equipment, this paper adopts 2-D plane set geometry theory. Single bearing measurement is converted into fan-shaped error region, and convex-polygon intersection-localization region of interference source is constructed by intersecting fan-shaped regions from multiple detection points. The pairwise Euclidean distances between all vertices of localization polygon are calculated to obtain regional diameter. This paper focuses on judging whether the circle taking the line connecting the two farthest points as diameter can fully contain the localization polygon. Numerical example shows that the polygon diameter only reflects maximum spatial span of the region, and the circle with this diameter cannot guarantee full coverage. In the given case, the diameter of localization polygon is 34.905 m, while the minimum enclosing-circle radius 17.455 m is larger than the diameter-derived circle radius 17.452 m, where some vertices lie outside the circle. It is verified that coverage judgment must be completed by vertex-by-vertex inspection or solving the minimum enclosing circle. Without probability assumptions, the proposed geometric modeling provides theoretical support for automatic localization of interference sources using direction-finding sensors carried by robot-dogs.
Keywords: Radio interference source; Bounded direction-finding error; Intersection localization; Convex polygon; Minimum enclosing circle

1 INTRODUCTION

Passive localization of radio interference sources is an important research topic in the field of electromagnetic spectrum monitoring. Robots equipped with direction-finding sensors can complete automatic interference-source inspection in hazardous scenarios, effectively overcoming the drawbacks of low efficiency and high personal-safety risks of manual inspection [1-2]. Practical direction-finding devices generally suffer from bounded angular errors. Such errors convert a single bearing reading into a fan-shaped uncertainty region. Intersection of fan-shaped regions from multiple detection points forms a complex convex-polygon solution set. Geometric description and coverage judgment for this solution set directly determine whether subsequent elimination tasks can be performed safely [3-4]. Research on geometric characteristics of intersection-localization solution sets under bounded-error conditions provides significant engineering support for autonomous localization of interference sources on robot platforms [5].

Extensive achievements have been made in bearing-only passive localization. Most existing studies adopt probability-assumptive methods such as least-squares and Kalman filtering to obtain point-estimated target coordinates under Gaussian random-noise conditions [6-7]. For measurement noise with unknown-but-bounded bounds, set-membership estimation can output the complete feasible position set of targets without pre-defining noise probability distributions [8-9]. Nevertheless, most existing literature focuses on ellipsoidal outer-bound set-membership state recursion, while seldom investigating convex-polygon solution sets yielded by multi-bearing fan-shaped region intersection. Moreover, the fundamental geometric judgment problem — whether the circle defined by the regional diameter can fully enclose the localization region — is frequently ignored, which may introduce implicit model errors in subsequent elimination-radius verification [10].

To fill the above-mentioned research gaps, this paper avoids probability-distribution assumptions and adopts two-dimensional set geometry. Bearing measurements are transformed into fan-shaped error regions, and the convex-polygon intersection-localization region is constructed via intersection operations of multi-sensor fan-shaped regions. Pair-wise Euclidean distances of all polygon vertices are calculated to acquire the region diameter. Two coverage-judgment approaches including vertex-by-vertex inspection and minimum-enclosing-circle solving are proposed. Numerical examples reveal that the polygon diameter cannot be directly treated as the diameter of the minimum enclosing circle. The presented work provides underlying geometric-model support for localization-elimination co-simulation of radio-interference sources on robot-dog platforms.

© By the Author(s) 2026, under the CC BY-NC-ND license (http://creativecommons.org/licenses/by-nc-nd/4.0).

2 METHODOLOGY

2.1 Intersection Localization Model under Bounded Bearing Errors

The bearing measurement provided by the direction-finding equipment contains an error of no more than 1°. Therefore, the real interference source from a single measurement should be confined within a fan-shaped region bounded by two boundary rays, rather than along a single ray defined by the bearing reading. If measurements are performed at multiple positions, the interference source must satisfy all measurement constraints simultaneously. Thus, the intersection of all fan-shaped regions constitutes the localization region.

This problem first constructs an intersection localization polygon model based on detection point coordinates and bearing measurements. Then it calculates the diameter of this polygon and provides constraint conditions to judge whether the circle with this diameter can fully cover the entire localization region. To avoid introducing unnecessary probability assumptions, this paper directly establishes a geometric model using the upper and lower error bounds given in the problem.

2.1.1 Determination of bearing range for a single detection point

Since the absolute value of bearing error does not exceed 1°, a bearing reading is first extended to the interval where the true bearing angle may lie:

$$\theta_i \in [\hat{\theta}_i - \alpha, \hat{\theta}_i + \alpha], \quad \alpha = 1^\circ \tag{1}$$

where $\hat{\theta}_i$ denotes the bearing measured at the i-th detection point; θ_i is the true bearing angle of the interference source relative to this detection point; α is the maximum direction-finding error. Angles exceeding 360° or less than 0° are processed modulo 360°. Figure 1 shows a schematic diagram of the bearing error region.

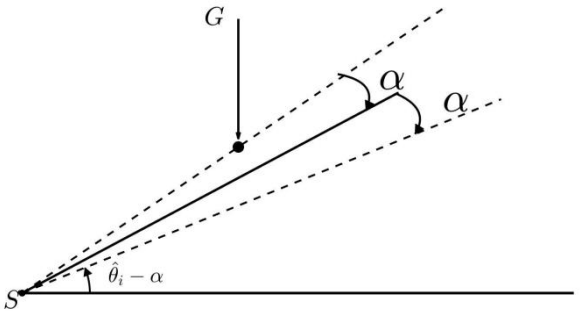


Figure 1 Schematic Diagram of Bearing Error Region

The geometric meaning of Equation (1) is illustrated in Figure 1. The dashed lines in the figure represent the error interval where the true bearing angle may fall, and the fan-shaped area between the two boundary rays is the allowable direction range of the interference source for this measurement.

To map the angular interval in Equation (1) onto the plane coordinate system, rays are drawn from the detection point along the two endpoints of the interval:

$$\vec{r}_i^{\pm}(t) = s_i + t\begin{bmatrix}\cos(\hat{\theta}_i \pm \alpha)\\ \sin(\hat{\theta}_i \pm \alpha)\end{bmatrix}, \quad t \geq 0 \tag{2}$$

where $s_i = (x_i, y_i)^T$ is the coordinate of the i-th detection point; $\vec{r}_i^{-}(t)$ and $\vec{r}_i^{+}(t)$ denote the lower and upper boundary rays of the bearing interval, respectively; t is a non-negative distance parameter on the ray. The region between the two rays is denoted as W_i, representing the allowable positions of the interference source for the i-th measurement.

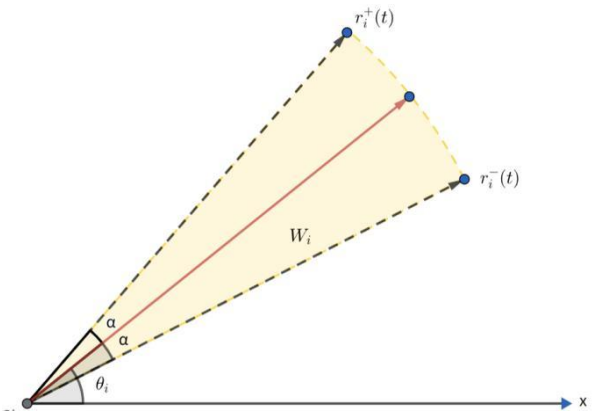


Figure 2 Schematic Diagram of Bearing Error Fan for a Single Detection Point

According to Equation (2), rays drawn from the detection point along the two boundary rays form a fan-shaped region on the plane, as shown in Figure 2. This figure further clarifies the possible direction range of the interference source in a single measurement, which serves as an important geometric object for solving the intersection of multiple measurements to obtain the localization region.

Figure 2 shows the conversion of the angular interval in Equation (1) into a fan-shaped region on the plane. The fan-shaped region is denoted as W_i, where i represents the allowable positions of the interference source for the i-th measurement. When multiple detection points exist, the localization region of the interference source can be obtained by computing the intersection of all fan-shaped regions.

2.1.2 Localization region for multiple monitoring points

Since the real interference source must satisfy every measurement simultaneously, the localization region is actually the intersection of the error fan-shaped regions corresponding to the bearing measurements of each detection point. Its set can be expressed as the following intersection:

$$P = \bigcap_{i=1}^{n} W_i \tag{3}$$

where n is the number of valid detection points; P is the localization region of the interference source.

In numerical solution, the intersection points of each fan boundary line are calculated sequentially. Only intersection points lying within all W_i are retained. After removing duplicate points, the remaining points are sorted counterclockwise to obtain the vertices $V_1, V_2, ..., V_m$ of the localization polygon, where m is the number of polygon vertices.

If the intersection is empty, the measurement results are inconsistent. If the intersection is unbounded, the intersection angle between detection points is too small, and it is necessary to change detection positions or add another measurement.

2.1.3 Geometric expression of localization region

Next, the vertices of the localization polygon are determined by calculating the intersection points between different boundary rays. Let boundary rays L_a and L_b start from detection points S_a and S_b, with direction vectors $\vec{u}_a$ and $\vec{u}_b$, respectively. The intersection point of the two boundary rays can be determined by the following formula:

$$S_a + t_a\vec{u}_a = S_b + t_b\vec{u}_b,\ V_{ab} = S_a + t_a\vec{u}_a,\ t_a, t_b \geq 0 \tag{4}$$

where S_a and S_b are the starting points of the two boundary rays; $\vec{u}_a$ and $\vec{u}_b$ are the corresponding unit direction vectors; t_a and t_b are distance parameters from the intersection point to the two detection points; V_{ab} is the intersection point of the two boundary rays. When both t_a and t_b are no less than 0 and the intersection point satisfies the remaining bearing fan constraints, V_{ab} is a valid polygon vertex.

Considering that the polygon diameter is the maximum distance between any two points within the region, and the region is a convex polygon, the two farthest points must be polygon vertices. Therefore, the distances between all vertices are calculated:

$$d_{pq} = \sqrt{(x_p - x_q)^2 + (y_p - y_q)^2},\quad D = \max_{1\leq p\leq q\leq m} d_{pq} \tag{5}$$

where $V_p = (x_p, y_p)$ and $V_q = (x_q, y_q)$ are any two polygon vertices; d_{pq} is the Euclidean distance between these two vertices; D is the diameter of the localization polygon.

When the number of vertices is small, directly comparing all C_m^2 groups of distances yields simple calculation without approximation errors. Direct comparison is adopted in this problem due to the limitation of the target region. However, when the number of vertices is large, the rotating calipers method can accelerate the calculation.

2.2 Coverage Judgment Model for Diameter Circle

Let the two vertices with maximum distance D be V_p and V_q. To test the circle with the line segment connecting these two farthest vertices as the diameter, the center and radius are calculated first:

$$C = \frac{V_p + V_q}{2},\quad R = \frac{D}{2} \tag{6}$$

where C is the center of the diameter circle; R is the radius of the diameter circle. Since both the disk and the localization region are convex sets, it is only necessary to check whether all vertices fall inside the circle. For this purpose, the maximum distance from each vertex to the circle center is calculated:

$$r_{max} = \max_{1\leq j\leq m} \| V_j - C\|_2 \tag{7}$$

where r_{max} is the maximum distance from all polygon vertices to the center C; $|\cdot|_2$ denotes the Euclidean distance on the plane. Based on the magnitude relationship between the maximum vertex distance and the circle radius, the coverage conclusion can be directly obtained:

$$\begin{cases} r_{max} \leq R, & the diameter circle can cover the localization region \\ r_{max} > R, & the diameter circle cannot cover the localization region \end{cases} \tag{8}$$

When $r_{max} > R$, at least one vertex lies outside the circle, so the entire localization region cannot be fully covered by this circle. To judge whether there exists a circle with diameter equal to D that can cover the localization region, the minimum enclosing circle of the localization polygon also needs to be calculated:

$$R_{min} = \min_{c} \max_{1\leq j\leq m} \|V_j - c\|_2 \tag{9}$$

where c is the circle center to be selected; R_{min} is the radius of the smallest circle that can cover all vertices. A minimum enclosing circle is determined by at most two or three boundary vertices, so it can be solved by enumerating vertex pairs and vertex triplets.

It can be seen that the polygon diameter only represents the distance between the two farthest points in the region and cannot guarantee that a circle with radius D/2 can cover the entire region. For example, an equilateral triangle with side length D has a diameter of D, but its circumscribed circle radius is $D/\sqrt{3} > D/2$. Therefore, a circle with diameter D cannot cover this triangle.

3 RESULTS

3.1 Calculation-Case Parameter Setting

Two detection points are selected for calculation. Their coordinates, bearing readings and true bearing intervals are shown in Table 1.

Table 1 Input Parameters for the Two-Point Direction-Finding Case

Detection Point	x / m	y / m	Bearing / °	True Bearing Interval / °
s_1	-500	0	44.5	[43.5,45.5]
s_2	500	0	135.5	[134.5,136.5]

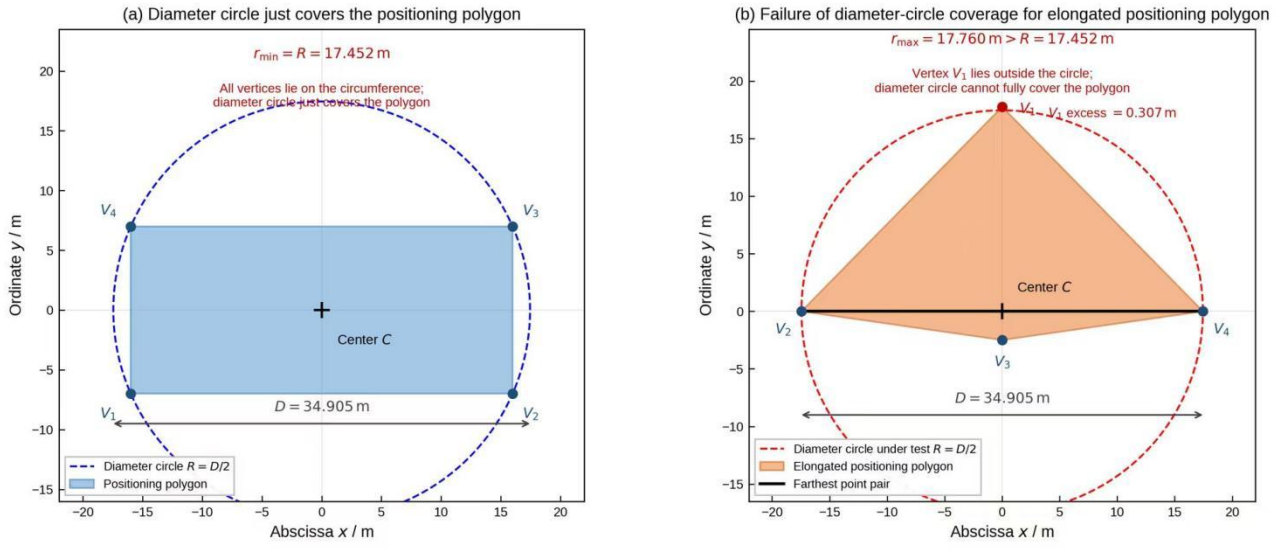
To simultaneously display the polygon geometric information and the coverage status of the diameter circle, the distances from each vertex to the center C = (0,491.044) are listed in Table 2. The coordinates of the four vertices are V_1, V_2, V_3, V_4, respectively.

Table 2 Localization Polygon Vertices and Diameter Circle Coverage Inspection

Vertex	Coordinate / m	Distance to Center C / m	Comparison with R = 17.452	Position Judgment
V_1	(0.508,804)	17.760	> R	Outside circle
V_2	(-17.452,491.044)	17.452	= R	On circumference
V_3	(0,474.482)	16.562	< R	Inside circle
V_4	(17.452,491.044)	17.452	= R	On circumference

3.2 Calculation of Localization-Polygon Diameter and Diameter-Circle Coverage Verification

Substitute the selected two detection points into the intersection localization model for solution. The visualization of the obtained polygon localization region and whether the circle corresponding to its diameter can achieve coverage is shown below. Figure 3 is a schematic diagram illustrating the localization of polygon vertices and the farthest vertex.



(a) (b)

Figure 3 Schematic Diagram of Localization Polygon Vertices and Farthest Vertex Pairs. (a) Diameter circle just covers the positioning polygon; (b) Failure of diameter circle coverage

It can be seen from Figure 3 that the four vertices form a convex quadrilateral, and the farthest vertex pair needs to be determined by comparing the distances of all vertex pairs.

Substitute the six groups of distances between the four vertices into Equation (5):

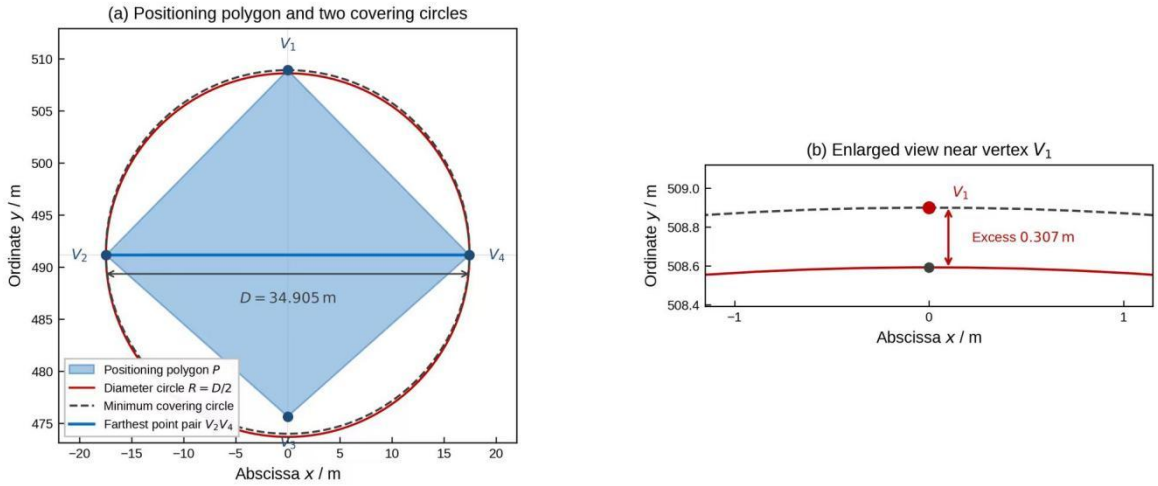
$$D = \|V_2 - V_4\|_2 = 34.905\,m \tag{10}$$

From Equation (7), the center of the diameter circle is C = (0,491.044),m and the radius is R = 17.452,m. Then compare the maximum distance from vertices to the center with the radius to judge coverage:

$$r_{max} - R = 17.760 - 17.452 = 0.307\,m > 0 \tag{11}$$

where $r_{max} - R$ denotes the out-of-circle excess. Its positive value indicates that vertex V_1 lies outside the diameter circle. Therefore, this diameter circle cannot cover the entire localization region.

To clearly judge whether the diameter circle can cover the whole localization region, the geometric relationship between the circle and the polygon is plotted as Figure 4.



(a) (b) Enlarged view near vertex V_1

Figure 4 Two-Point Intersection Region and Diameter Circle Coverage Judgment. (a) Positioning polygon and two covering circles; (b) Enlarged view near vertex V_1

It can be observed from Figure 4 that vertex V_1 is obviously outside the diameter circle, visually verifying the conclusion of coverage failure. Further calculation shows that the minimum enclosing circle radius of this quadrilateral is 17.455,m, which is still greater than D/2. This means that even if the circle center is reselected, there is no circle with diameter exactly D that can cover the entire localization region. Key results are summarized in Table 3. The "diameter circle" in the table refers to the circle constructed with the farthest points as the diameter.

Table 3 Main Calculation Results

Index	Calculated Value	Judgment Function
Localization polygon diameter D	34.905 m	Gives the maximum span within the region
Diameter circle radius R = D/2	17.452 m	Constructs the circle to be inspected
Maximum vertex distance r_{max}	17.760 m	Larger than R, vertices exist outside the circle
Out-of-circle excess $r_{max} - R$	0.307 m	Indicates coverage failure of the diameter circle
Minimum enclosing circle radius R_{min}	17.455 m	Still larger than D/2
Final Conclusion	Cannot cover	The circle with diameter D cannot cover the localization region of this case

In this problem, the convex polygon localization region of the interference source is determined by the intersection of multiple bearing fan-shaped regions through geometric transformation. The diameter of the localization region is obtained by enumerating the Euclidean distances between all vertex pairs.

The algorithm demonstrates that a circle with the diameter of the localization region as its diameter cannot necessarily cover the localization region. Vertex coverage inspection or minimum enclosing circle calculation must be further performed.

4 CONCLUSIONS

This paper constructs an intersection-localization geometric model for radio interference sources under bounded direction-finding errors without probability-distribution assumptions. By intersecting fan-shaped uncertainty regions from multiple detection points, the convex-polygon feasible localization region is obtained. A complete set of calculation procedures for polygon diameter, vertex-by-vertex inspection and minimum enclosing-circle solving is proposed to judge coverage performance. Numerical case results verify that the diameter of the convex localization polygon cannot be directly used as the diameter of the covering circle. Even if all pairwise vertex distances are calculated, additional

minimum enclosing-circle computation is indispensable for reliable safety judgment. The presented geometric-driven modeling can provide theoretical support for robot-dog-borne direction-finding sensors to implement autonomous interference-source searching and elimination, and possesses application feasibility for spectrum-monitoring simulation scenarios with strict safe-clearance distance constraints.

Nevertheless, the current study still has several limitations. The research is confined to ideal two-dimensional line-of-sight conditions; signal occlusion. Future research will extend the geometric model to handle non-ideal measurement conditions with outlier bearings, and further combine sensor-placement optimization algorithms to realize joint optimization of detection-point layout and localization-region quality. Moreover, field measured data will be adopted to validate the model, so as to promote the transformation from pure geometric simulation to practical engineering application for radio-interference-source monitoring.

COMPETING INTERESTS

The authors have no relevant financial or non-financial interests to disclose.

REFERENCES

[1] Chen S, Liang B. Radio Frequency Interference Detection Using Swin Transformer Embedding U2-Net. Advances in Astronomy, 2025, 2025(1): 3232269.

[2] Nazri A A, Abidin Z Z, Sabri M R M, et al. Temporal variability in low-frequency radio interference: Insight from high-cadence monitoring at a candidate radio notification zone in Malaysia. Advances in Space Research, 2025, 76(3): 1832-1853.

[3] Malik A, Rao M. Radio Frequency Interference, Its Mitigation and Its Implications for the Civil Aviation Industry. Electronics, 2025, 14(12): 2483.

[4] Nguyen K T, Nguyen D N, Nguyen Q H, et al. Signal Enhancement and Interference Reduction with Minimum-Variance Distortionless Response Algorithm Using MATLAB and GNU Radio Simulations. Engineering Proceedings, 2025, 92(1): 73.

[5] Calkins M L. British surveillance of postwar Soviet radio jamming: US–UK intelligence relations and interference detection at BBC Tatsfield, 1948-1949. Journal of Intelligence History, 2025, 24(2): 162-183.

[6] Munshi S, Mertens F G, Koopmans L V E, et al. Near-field imaging of local interference in radio interferometric data: Impact on the redshifted 21 cm power spectrum. Astronomy & Astrophysics, 2025, 697: A203.

[7] Sophan S, Supnithi P, Myint M M L, et al. Statistical analysis and effects of radio frequency interference in GPS signal quality in Thailand. GPS Solutions, 2024, 28(4): 194.

[8] Zheng F, Zhang Z, Zhang D. Lightweight deep neural network for radio frequency interference detection and segmentation in synthetic aperture radar. Scientific Reports, 2024, 14(1): 20685.

[9] Luo Z, Li J, Song T, et al. Range-Doppler image classification for interference detection in over-the-horizon radar. Digital Signal Processing, 2024, 155: 104727.

[10] Knowles K, An F, Datta A, et al. The future of radio astronomy in an increasingly crowded spectrum – Present and expected science in radio continuum astrophysics. Proceedings of the International Astronomical Union, 2024, 20(A32): 177-180.